Experimental Investigation of a Novel High Energy Density Mobile Sorption–based Thermal Battery

Lingshi Wang[1], Xiaobing Liu[1], Zhiyao Yang[1,2], Kyle R. Gluesenkamp[1]

[1]Oak Ridge National Laboratory, Oak Ridge, TN 37831, U.S.A.

[2]Lyles School of Civil Engineering, Purdue University, West Lafayette, IN 47906, U.S.A.

Keywords

Mobile sorption-based thermal battery, crystallization, dissolution, energy storage density, experimental investigation

ABSTRACT

Around 20% of the total primary energy use in the United States is for thermal demands of buildings, such as space cooling, dehumidification, and space heating. Low-grade geothermal energy is abundant and could effectively satisfy these thermal demands. However, low-grade geothermal energy is underused because geothermal fluids have an energy density too low to justify transportation between the existing resources and buildings. The mobile sorption-based thermal battery (MSTB) system was thus developed to store the low-temperature heat using three-phase (vapor-liquid solution-solid crystal) sorption technology with a much higher energy density than a geothermal fluid provides. The energy density of an MSTB is over 6 times that of conventional hot water, enabling economical long-distance transport of low-temperature heat for thermal end uses. This can alleviate peak demand on the electricity grid by offsetting space-conditioning loads, improving the reliability and resilience of US energy systems. High energy density, fast crystallization, and crystal dissolution of the sorption material are critical to the viability and performance of the MSTB system. Therefore, the design and operation of MSTB systems must ensure effective generation and dissolution of the salt crystals inside the MSTB. To achieve this target, this study developed a prototype MSTB and its testing apparatus, and experimentally investigated the prototype MSTB. The crystallization and dissolution performance were also theoretically defined and quantified. The experimental results showed that the prototype MSTB was able to achieve an energy storage density of 903.0 kJ/kg and a

maximum discharge rate of 1.3 kW. This study proves the feasibility and high performance of the MSTB concept, which is helpful to further study and development of the MSTB system.

1. Introduction

Buildings consume over 40% of the total primary energy used in the United States, of which 40–70% is for thermal demands such as space heating, cooling, and water heating. Low-grade geothermal energy is abundant and could effectively satisfy those thermal demands. However, the current use of geothermal resources is limited because of the distance between the existing resources and potential end uses such as large buildings. The existing direct use of low-temperature (<150°C) hydrothermal energy is highly localized and relatively small in scale because the energy density of hot water is too low to justify the cost of long-distance transport. Another underused geothermal resource is the heat contained in the 25 billion barrels of geothermal fluid (mostly water), at temperatures of up to 150°C, co-produced at oil and gas wells in the United States each year (DOE 2015), which is typically all wasted.

Facing the spatial mismatch of energy resource and demand, a mobile thermal storage system with high energy density to enable economic long-distance transportation is thus highly desired. Previous studies by a team at Oak Ridge National Laboratory (Liu et al. 2015; Yang et al. 2016) calculated and compared the energy densities and economics of existing and potential technologies for storing and transporting low-temperature geothermal energy for thermal end uses. Unlike conventional stationary thermal storage systems designed only to deal with the temporal mismatch of the thermal resource and demand, the energy density of a mobile thermal storage system is critical to its viability and performance. Therefore, conventional systems have not been able to provide sufficient energy density to justify transport. Conventional systems include use of the sensible heat of chilled or hot water (Nelson, 1999) and the fusion heat of ice and other phase-change-materials (Cabeza, 2011). On the other hand, new system concepts based on sorption technology using the vaporization heat of water have been proposed for mobile storage (Liu et al. 2015; Yang et al. 2016) and stationary seasonal storage (N'Tsoukpoe et al. 2013, 2014). The seasonal storage system used concentrated salt solution to store solar heat with minimum loss during long storage periods. It allows some salt crystallization in the storage tank to achieve a high energy density. The mobile storage system targeted maximal energy density by using primarily salt crystals as the storage material.

The concept of a mobile sorption-based thermal battery (MSTB) system was thus developed using three-phase (vapor-liquid solution-solid crystal) sorption technology to store low-temperature heat at very high energy density, allowing economical long-distance transport while also providing versatile end uses. The design of an MSTB is shown in Figure 1. The MSTB system includes a charging system (generator), thermal battery (MSTB), and discharging system (desiccant-evaporative cooler). At the geothermal charging site, the system uses heat from a low-temperature (<150°C) geothermal resource site to dehydrate and concentrate an aqueous salt solution, such as LiCl or LiBr. The concentrated solution then flows into the MSTB, where it is cooled to allow salt in the solution to crystallize into hydrate crystals. While the salt crystals accumulate in the MSTB, the remaining liquid solution circulates back into the regenerator for further reconcentration. Once the MSTB is filled with salt hydrate crystals, it can be decoupled from the generator and transported to distant buildings or industrial plants. At the end use site, the MSTB is connected to an absorption system to release the energy stored in the crystals. The

diluted solution exiting the absorption system flows into the MSTB and dissolves the salt crystals, and the reconcentrated solution flows back into the absorption system to support continuous generation of heating and cooling without any heat input. Once all crystals in the MSTB are exhausted, the tank is transported back to the geothermal site for regeneration and another cycle of operation.

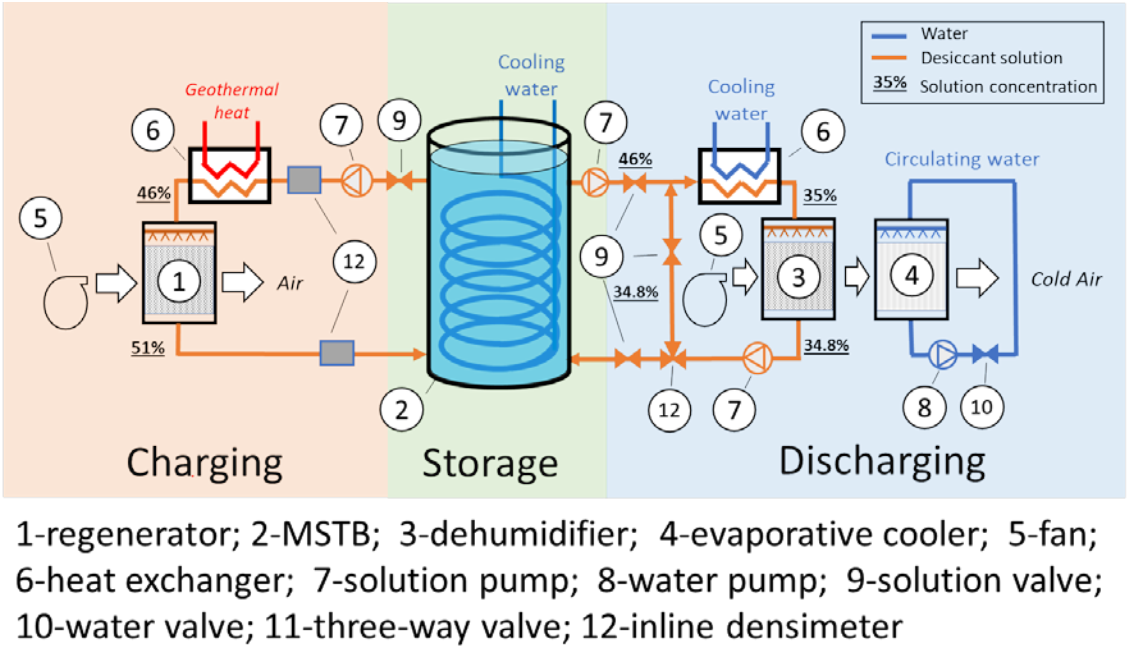

Figure 1: Proposed mobile sorption-based thermal battery system.

The high energy density for an MSTB is mainly determined by the crystallization performance. Therefore, the characteristics of the crystals in the solution environment are crucial information for designing the MSTB system. Similarly, timely dissolution of crystals is needed for continuous operation of an MSTB with sufficient cooling/heating output. The dynamic characterization of salt (LiCl and LiBr) crystallization and dissolution provides valuable information not only for the MSTB but for all sorption-based high-energy-density thermal storage. The component design determines the effectiveness and reliability of the MSTB. A lab-scale prototype of a seasonal storage system developed by N'Tsoukpoe (2013) was used to evaluate component designs for confining crystallization in the MSTB. However, this seasonal storage system was designed to allow crystals in the storage tank, rather than targeting fast and effective crystallization and dissolution. Therefore, an experimental apparatus was developed in this study to characterize the crystallization and dissolution of an energy storage solution. The MSTB was evaluated through lab tests to achieve the needed crystal generation and dissolution performance. The evaluation method for crystallization and dissolution performance was analyzed. Crystallization and dissolution tests in the experimental apparatus were conducted. Finally, the energy storage density and discharge rate were obtained based on the test results.

2. Experimental Apparatus for Characterizing crystallization and Dissolution

To develop the MSTB, especially achieve the required energy storage density and charge/discharge rate, the first priority was understanding the characteristics of the crystallization/dissolution processes in the MSTB. Thus, an experimental apparatus for characterizing the crystallization and dissolution of an energy storage medium was developed, as shown in Figure 2. The experimental apparatus included one MSTB (5 L capacity) and two solution tanks (10 L capacity for each). The energy storage medium adopted in this study was an LiCl aqueous solution. The crystallization and dissolution of the LiCl aqueous solution occurred only in the MSTB.

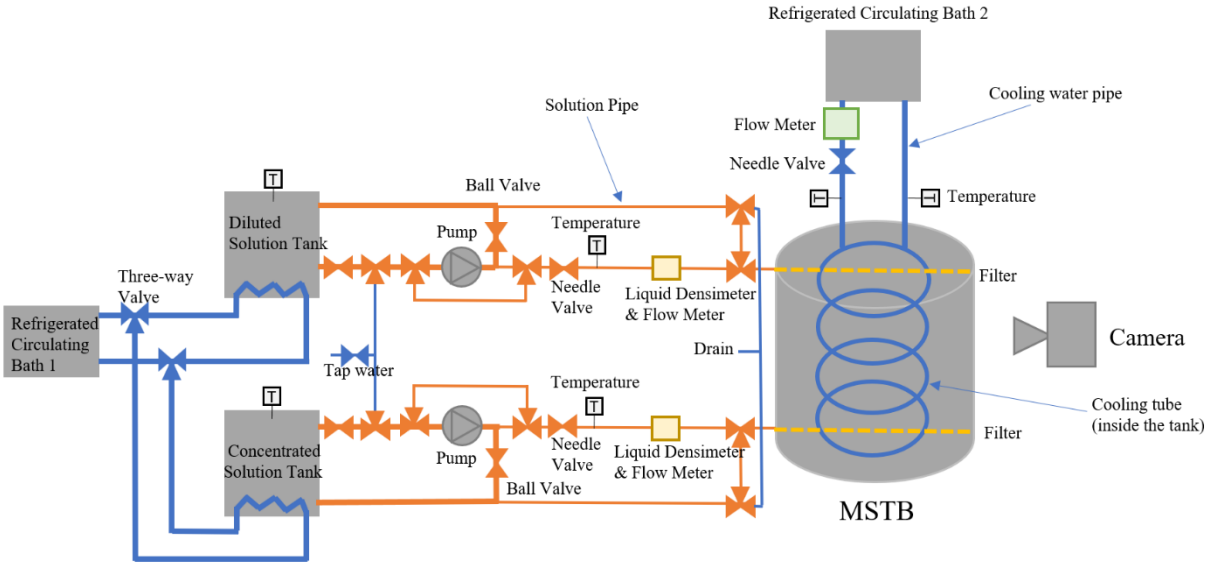

Figure 2: Schematic of experimental apparatus for characterizing the crystallization and dissolution of energy storage medium.

To characterize the crystallization process, the hot and concentrated solution from the concentrated solution tank was pumped into the MSTB. Then it was cooled by a refrigerated circulating bath to crystallize on the surface of the cooling coil in the MSTB. As salt crystals were generated, the remaining liquid solution in the MSTB became dilute and was pumped to the dilute solution tank. With a concentrated solution incoming and a diluted solution outgoing, the amount of crystals in the MSTB increased until a maximum was reached. To characterize the dissolution process, the warm and diluted solution from the diluted solution tank was pumped into the MSTB, where it dissolved the salt crystals in the MSTB. The salt concentration of the liquid solution in the MSTB increased and the concentrated solution was pumped into the concentrated solution tank. The temperatures of the solution in the three tanks were controlled by the circulating baths with cooling and heating functions. The flow rate of the solution was manually adjusted with a needle valve.

The inlet and outlet temperatures of the salt solution and cooling water in the MSTB were measured by resistance temperature detectors, and the temperature of the solution in the tanks

was measured by T-type thermocouples. The flow rate of the cooling water was measured by an electromagnetic flowmeter, and the flow rate and density of the solution were measured by two Micro Motion Coriolis flow and density meters. A camera was used to visually record the crystallization/dissolution process. The specifications of the instruments are listed in Table 1.

To prevent unwanted crystallization in tubes connecting the tanks and in the circulation pumps, a water flushing system was added, as shown in Figure 2. When the experiment was finished, tap water was used to flush the tubes and pumps until the densimeter reading dropped to 1 g/cm^3.

Table 1: Instrumentation

Measured value	Instrument	Range	Uncertainty
Temperature of salt solution and cooling water	Resistance temperature detector [Omega PR-20 Series, Class "A" DIN]	–50 to 260°C (instrument range)	±0.15°C
Temperature of solution in the tanks	T-type thermocouple probes [Omega]	–270 to 370°C	±0.5°C
Flow rate of cooling water	Electromagnetic flow meter [QSE05NPT09]	0.1–10 GPM (instrument range)	±0.5% of rate
Flow rate of solution	MicoMotion ELITE CMFS010H Coriolis	0–110 L/h (instrument range)	±0.05% of rate
Density of solution	MicroMotion ELITE CMFS010H Coriolis	0–4000 kg/m3	±0.2 kg/m3

3. Evaluation on Crystallization and Dissolution Performance

The performance of the MSTB can be evaluated with two indicators: the energy storage density (ESD) and the discharge rate (Q_d). ESD is the performance index of the MSTB, while Q_d depends not only on the MSTB but also on the associated discharging systems.

ESD is calculated with Eq. (1):

$$ESD = \frac{M_w\, q_v}{M_{s,d}} \quad (1)$$

where $M_{s,d}$ is the mass of the diluted halide salt solution after discharging process (kg), M_w is the mass of water released from the diluted solution after the charging process (kg), q_v is the latent heat of vaporization per unit mass of water (kJ/kg).

The mass balance equation of the water release process is shown as Eq. (2).

$$\left(M_{s,d} - M_w\right)(1 - X_e) + M_w = M_{s,d}(1 - X_d) \quad (2)$$

where X_e is the equivalent solution concentration after the charging process (–), X_d is the solution concentration after the discharging process, the value of X_d in a typical liquid desiccant dehumidifier is 0.35.

Combining Eqs. (1) and (2), ESD can be calculated with Eq. (3):

$$ESD = \frac{X_e - X_d}{X_e} q_v \quad (3)$$

The equivalent solution concentration (X_e) is calculated by Eq. (4):

$$X_e = \frac{M_{solute}}{M_s} = \frac{M_c X_c + (V_f - M_c/\rho_c)\rho_f X_f}{(V_f - M_c/\rho_c)\rho_f + M_c} \quad (4)$$

where M_{solute}, M_s, M_c, X_c, ρ_c are the total mass of solute (kg), the total mass of solid-liquid mixture (kg), the total mass (kg), the equivalent concentration (–) and density (kg/m^3) of salt crystals generated in the MSTB, respectively; the crystals could be monohydrate or dihydrate depending on the cooling temperature (Conde, 2004), V_f is the final total volume of the solid-liquid mixture in the MSTB (m^3); X_f, ρ_f are the final concentration (–), density (kg/m^3) of the remaining solution in the MSTB, respectively.

The calculation of total mass of salt crystals (M_c) is as follows.

The mass balance in the MSTB during crystallization process is shown in Eq. (5):

$$\int_{t_i}^{t_f}(m_{in} - m_{out})dt = \left(V_f - \frac{M_c}{\rho_c}\right)\rho_f + M_c - V_i\rho_i \quad (5)$$

where t_i and t_f represent the initial and final time (s), respectively; m_{in} , m_{out} represent the mass flow rate of inlet solution and outlet solution (kg/s), respectively; V_i, ρ_i represent the volume (m^3) and density of the solution (kg/m^3) in the MSTB at the initial time, respectively.

The mass balance of halide salts in the MSTB during crystallization process is shown in Eq. (6):

$$\int_{t_i}^{t_f}(m_{in}X_{in} - m_{out}X_{out})dt = M_c X_c + \left(V_f - \frac{M_c}{\rho_c}\right)\rho_f X_f - V_i\rho_i X_i \quad (6)$$

where X_{in} , X_{out}, X_i represent the concentration (–) of inlet solution and outlet solution, solution in the MSTB at the initial time, respectively.

Let

$$A = \int_{t_i}^{t_f}(m_{in} - m_{out})dt \quad (7)$$

$$B = \int_{t_i}^{t_f}(m_{in}X_{in} - m_{out}X_{out})dt \quad (8)$$

Assuming that (1) the solution in the MSTB is well mixed, so the state of the outlet solution is the same as that of the solution in the MSTB; and (2) the volume of the solid-liquid mixture in the MSTB doesn't change, then the following equations can be obtained.

$$X_i = X_{in,i}\ ,\ \rho_i = \rho_{in,i} \quad (9)$$

$$X_f = X_{out,f}\ ,\ \rho_f = \rho_{out,f} \quad (10)$$

$$V_i = V_f = V \quad (11)$$

where subscripts *i* and *f* represent the initial and final states of the solution in the MSTB, respectively; subscripts *in,i* and *out,f* represent the initial state of the inlet solution and the final state of the outlet solution, respectively.

Based on Eqs. (9), (10), and (11), Eq. (4) can be converted to Eq. (12):

$$X_e = \frac{V\rho_{out,f}X_{out,f}+(X_c-X_{out,f}\rho_{out,f}/\rho_c)M_c}{V\rho_{out,f}+(1-\rho_{out,f}/\rho_c)M_c} \quad (12)$$

Combining Eqs. (5), (6), (7) and (8) with Eqs. (9), (10), and (11), the total mass of salt crystals (M_c) can be calculated with Eq. (13):

$$M_c = \frac{(\rho_{out,f}X_{out,f}-\rho_{in,i}X_{in,i})A-(\rho_{out,f}-\rho_{in,i})B}{(\rho_{out,f}-\rho_{in,i})\left(\frac{X_{out,f}\rho_{out,f}}{\rho_c}-X_c\right)+(\rho_{out,f}X_{out,f}-\rho_{in,i}X_{in,i})(1-\frac{\rho_{out,f}}{\rho_c})} \quad (13)$$

A and B can be calculated with the measured density and flow rate of the solution. Combining Eqs. (3), (12), and (13), the ESD can finally be calculated.

The crystal fraction (i.e., the ratio of crystal mass to the mass in the MSTB) (F_c) in the MSTB after the crystallization process is calculated by Eq. (14):

$$F_c = \frac{M_c}{\rho_i V_i+A} = \frac{M_c}{\rho_{in,i}V+A} \quad (14)$$

The MSTB's discharge rate (Q_d) is used to evaluate the dissolution performance, when the discharging system uses the liquid desiccant solution dissolved from the MSTB. Q_d is actually the latent cooling capacity for dehumidifying air and can be calculated by Eq. (15).

$$Q_d = (\frac{m_{out}X_{out}}{X_d} - m_{out})q_v \quad (15)$$

4. Preliminary Results and Discussion

4.1 Crystallization Test Results

A crystallization test was conducted in the MSTB. A strong solution with a concentration of 50.3% and a flow rate of 2.04 g/s flowed into the MSTB for crystallization by active cooling. The solution was cooled with 20.4°C cooling water. Meanwhile, the diluted solution in the tank resulting from the crystallization of the salt flowed out of tank at the same flow rate.

Figure 3 shows the evolution of crystals over time during the crystallization test. It can be seen that the LiCl hydrate crystals were generated first on the surface of the cooling coil and the tank wall, as the temperature at these places was lower, and then the crystals accumulated in the tank. The crystals were fluffy, which is helpful for dissolution. More than half of the tank was occupied by the crystals within 30 min, and the tank was almost full of crystals after 40 min. The data measured during the crystallization test are shown in Figure 4. In this test, the inlet conditions of the LiCl solution and the cooling water were maintained at their initial settings. It can be seen from Figure 4a that the concentration of the solution leaving the MSTB was the same as the inlet solution concentration at the beginning, and then it dropped to ~1.5%, lower than that of the inlet solution. This indicated crystals were forming, resulting in dilution of the remaining solution in the MSTB.

Based on test results and the calculation method described in Section 3, the crystallization performance was evaluated as follows:

- The total mass of salt crystals (M_c) generated in the MSTB was 2.065 kg, and the mass percentage of the crystals in the MSTB was 34.4 %.
- The ESD was 903.0 kJ/kg.

The ESD can be increased by generating more salt crystals. Proposed methods for achieving this goal include changing the flow rate of the solution and changing the cooling water temperature, both of which need further study.

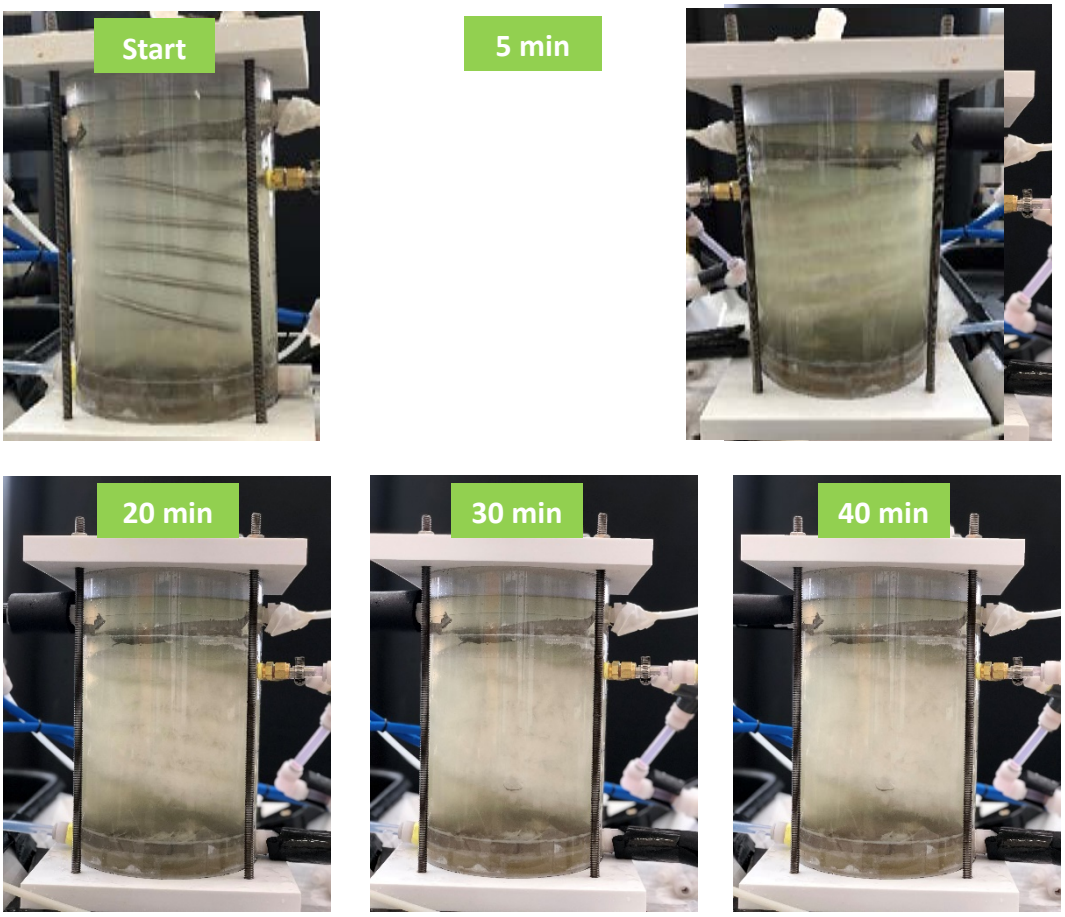

Figure 3: Crystallization process over time in the MSTB.

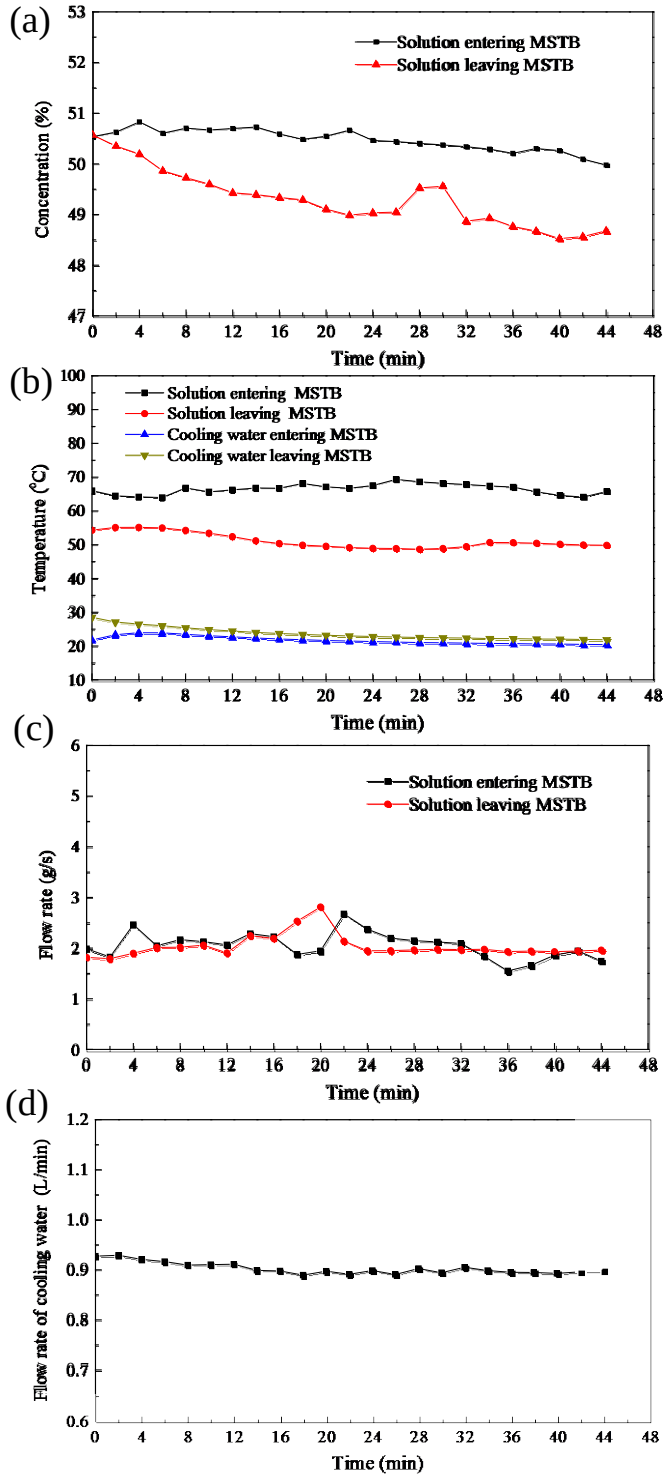

Figure 4: Measured data during crystallization process: (a) solution concentration, (b) temperature of solution and cooling water, (c) flow rate of solution, and (d) flow rate of cooling water.

4.2 Dissolution Test Results

A dissolution test was also conducted in the MSTB. The diluted solution with a concentration of 35.1% and a temperature of 40.9°C flowed into the MSTB to dissolve the crystals. The inlet condition of the diluted solution was a typical liquid desiccant condition after dehumidification. Meanwhile, the concentrated solution resulting from dissolving crystals flowed out of the MSTB. The inlet condition of the solution was kept constant to mimic the typical leaving condition of a LiCl solution after dehumidifying the air to a humidity ratio of 6–7 kg/kg. Both the inlet and outlet solution had an average flow rate of 5.9 g/s.

The dissolution process over time is shown in Figure 5. It can be seen that the LiCl hydrate crystals dissolved quickly. More than half of the crystals dissolved in 8 min, and almost all of them were dissolved in 16 min. The measured data during the dissolution test are shown in Figure 6. It can be seen from Figure 6a that the concentration of the solution leaving the MSTB was about 12 percentage points higher than that of the inlet solution at the beginning, and the difference gradually dropped to 5 percentage points in less than 20 min. These results indicated that the crystals dissolved quickly to increase the concentration of the solution entering the MSTB.

The discharge rate of the MSTB over time was calculated based on test results and the calculation method described in Section 3. The calculated result is shown in Figure 7. It shows that the prototype MSTB maintained a discharge rate of above 1 kW during the dissolution process, and the maximum discharge rate was as high as 1.3 kW. To further improve the discharge rate, proposed methods including changing the flow rate and the temperature of the inlet solution, which need further study.

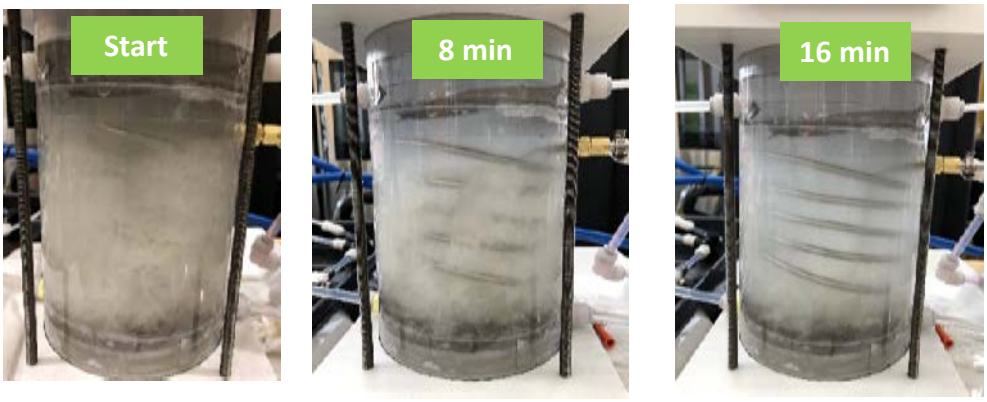

Figure 5: Dissolution process over time in the MSTB.

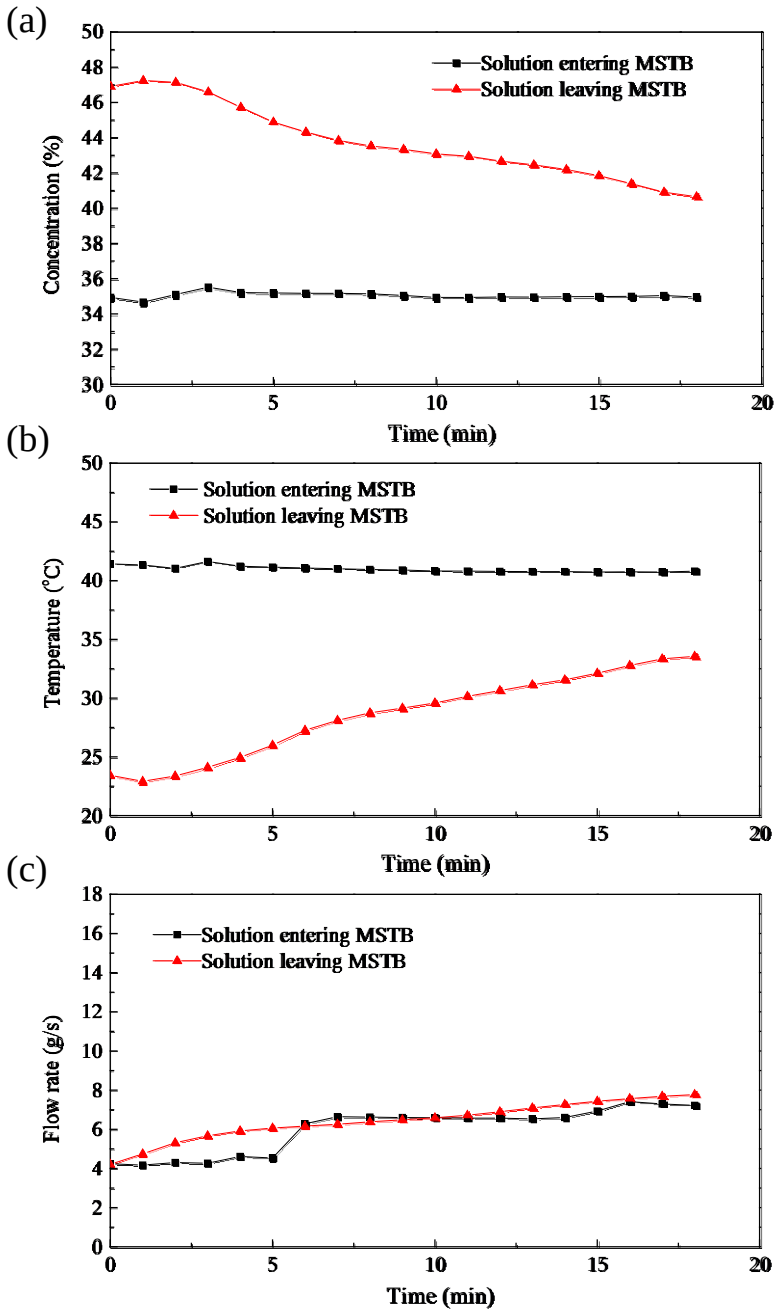

Figure 6: Measured data during dissolution process: (a) concentration of solution, (b) temperature of solution, (c) flow rate of solution.

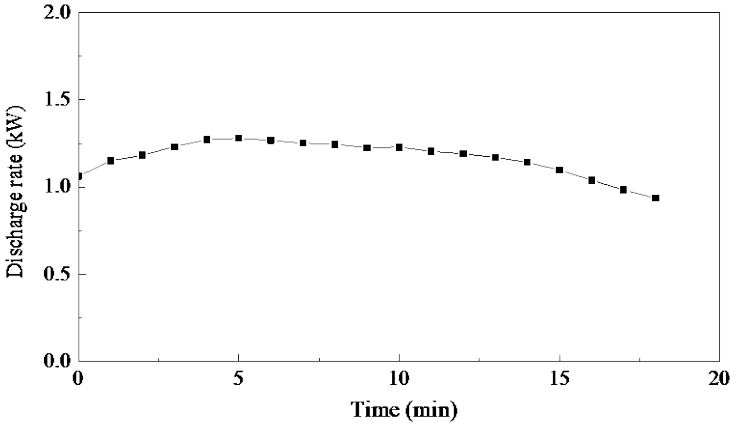

Figure 7: Calculated discharge rate of the MSTB based on dissolution test results.

5. Conclusions and Plan for Future Work

This paper presents an experimental study of the characteristics of crystallization and dissolution in an energy storage tank used for an MSTB system. An experimental test rig was developed for characterizing crystallization by active cooling and dissolution in the MSTB. A LiCl aqueous solution was used as the energy storage medium. Methods for calculating the ESD during the crystallization process and discharge rate during the dissolution process were derived. Preliminary tests of crystallization and dissolution of the MSTB were conducted. The crystallization results showed that the generated crystals are fluffy, and the MSTB, with an occupied volume of 4.3 L, can be filled with the generated salt crystals within 50 min. The ESD achieved in this study was 903.0 kJ/kg. The dissolution results showed that the LiCl hydrate crystals in the MSTB were fully dissolved in 16 minutes. The discharge rate was above 1 kW (equivalent latent cooling capacity for dehumidifying air) and the maximum discharge rate was up to 1.3 kW. These results demonstrate the feasibility of MSTB in high-density energy storage and thermal end uses.

To improve the MSTB performance, our future work will be devoted to increase the ESD and discharge rate using multiple methods, including increasing the solution flow rate, stripping the crystals on the surface of cooling coil, optimizing the design of the heat exchanger in the MSTB during the crystallization process, and optimizing the flow rate and temperature of the inlet solution to enhance the convection in the MSTB during the dissolution process.

Acknowledgment

This work was sponsored by the US Department of Energy's Geothermal Technologies Office under Contract No. DE-AC05-00OR22725 with UT-Battelle, LLC. The authors would also like to acknowledge Arlene Anderson and Joshua Mengers, US Department of Energy Geothermal Technologies Office.

REFERENCES

Cabeza, L. F., Castell, A., Barreneche, C. D., De Gracia, A., & Fernández, A. I. "Materials used as PCM in thermal energy storage in buildings: A review." *Renewable and Sustainable Energy Reviews*, 15(3), (2011),1675-1695.

Conde M.R. "Properties of aqueous solutions of lithium and calcium chlorides: Formulations for use in air conditioning equipment design." *Int J Therm Sci*, 43, (2004), 367–82.

DOE. "Direct Use of Geothermal Energy." *Available at http://energy.gov/eere/geothermal/direct-use-geothermal-energy*, (2015).

Liu, X., Yang, Z., Gluesenkamp, K. R., & Momen, A. M. "A Technical and Economic Analysis of an Innovative Two-Step Absorption System for Utilizing Low-Temperature Geothermal Resources to Condition Commercial Buildings." *ORNL/TM-2015/655*, Oak Ridge National Laboratory, Oak Ridge, TN (2015).

Nelson, J. E. B., Balakrishnan, A. R., & Murthy, S. S. "Parametric studies on thermally stratified chilled water storage systems." *Applied Thermal Engineering*, 19(1), (1999), 89-115.

N'Tsoukpoe, K. E., Le Pierrès, N., & Luo, L. "Experimentation of a LiBr–H2O absorption process for long-term solar thermal storage: Prototype design and first results." *Energy*, 53, (2013), 179-198.

N'Tsoukpoe, K. E., Perier-Muzet, M., Le Pierres, N., Luo, L., & Mangin, D. "Thermodynamic study of a LiBr–H2O absorption process for solar heat storage with crystallisation of the solution." *Solar Energy*, 104, (2014), 2-15.

Yang, Z., Liu, X., Gluesenkamp, K. R., & Momen, A. M. "A Preliminary Study on Innovative Absorption Systems that Utilize Low-Temperature Geothermal Energy for Air-Conditioning Buildings." *16th International Refrigeration and Air Conditioning Conference at Purdue*, Purdue University, West Lafayette, IN (2016).

Yang, Z., Liu, X., et al. "Transported Low Temperature Geothermal Energy for Thermal End Uses—Final Report." *ORNL/TM-2016/658*, Building Technologies Research and Integration Center (BTRIC), Oak Ridge National Laboratory (ORNL), Oak Ridge, TN (2016).